Journal of Power Sources 195 (2010) 779–786

Contents lists available at ScienceDirect

Journal of Power Sources

journal homepage: www.elsevier.com/locate/jpowsour

The bipolar plate of AISI 1045 steel with chromized coatings prepared by low-temperature pack cementation for proton exchange membrane fuel cell

Ching-Yuan Bai[a,*], Tse-Min Wen[b], Kung-Hsu Hou[c], Ming-Der Ger[a]

[a] Department of Chemistry and Materials Science and Engineering, Chung Cheng Institute of Technology, National Defense University, Tau-Yuan 335, Taiwan, ROC
[b] School of Defense Science, Chung Cheng Institute of Technology, National Defense University, Tao-Yuan 335, Taiwan, ROC
[c] Department of Power Vehicles and System Engineering, Chung Cheng Institute of Technology, National Defense University, Tao-Yuan 335, Taiwan, ROC

ARTICLE INFO

Article history:
Received 14 July 2009
Received in revised form 14 August 2009
Accepted 14 August 2009
Available online 22 August 2009

Keywords:
Low-temperature pack chromization
AISI 1045 carbon steel
Rolling
Electrical discharge machining
Interfacial contact resistance
Potentiodynamic test

ABSTRACT

The low-temperature pack chromization, a reforming pack cementation process, is employed to modify AISI 1045 steel for the application of bipolar plates in PEMFC. The process is conducted to yield a coating, containing major Cr-carbides and minor Cr-nitrides, on the substrate in view of enhancing the steel's corrosion resistance and lowering interfacial contact resistance between the bipolar plate and gas diffusion layer. Electrical discharge machining and rolling approach are used as the pretreatment to produce an activated surface on the steel before pack chromization process to reduce operating temperatures and increase deposition rates. The rolled-chromized steel shows the lowest corrosion current density, 3×10^{-8} A cm^{-2}, and the smallest interfacial contact resistance, 5.9 mΩ cm^2, at 140 N cm^{-2} among all tested steels. This study clearly states the performance of 1045 carbon steel modified by activated and low-temperature pack chromization processes, which possess the potential to be bipolar plates in the application of PEMFC.

1. Introduction

The development of fuel cells has received considerable attention in energy domains, because it is quieter, cleaner, and with higher transformation efficiency than a conventional internal combustion engine. Proton exchange membrane fuel cells (PEMFCs) are regarded as one of the most probable fuel cells for stationary and transportation applications in operating at low temperatures. Machined graphite composites are currently the most materials used as bipolar plates of PEMFCs [1]. However, the high cost for manufacturing a flow-field pattern in graphite and its brittleness are the major troubles in using this material for the widespread marketplace [2,3]. Therefore, metals have received attention recently to alternate graphite as bipolar plates, because the malleable and superior mechanical properties of metals allow to design a smaller and thinner stack to reduce the weight and volume of fuel cells. A number of metallic materials including aluminum [4], stainless steel [5,6], titanium [7], and copper alloys [8] have been investigated extensively to apply in bipolar plate of PEMFC. Nevertheless, the studies of carbon steels as bipolar plates were rare due to the poor corrosion resistance of these materials under atmosphere and solution environments.

Many previous literatures have been reported in producing diffusion coatings on various metals to enhance their surface characteristics by pack cementation process. Some examples, which executed such procedures on various alloys, are worth to take notice of the subjecting performance and operating temperature [9,10]. It can be seen that these previous studies were practiced at temperatures above 750 °C, and systematic investigation on chromizing carbon steels in the temperature range below 700 °C is almost non-existent according to our survey of literatures. In fact, the AISI 1020 steel had been conducted by a low-temperature pack chromization process with an activated pretreatment of electrical discharge machining in our previous examination [11]. The modified 1020 steels exhibited superior behavior, including measurements of corrosion and interfacial contact resistance, in a simulated PEMFC environment and possessed potential to be a candidate material for bipolar plates. In the work, it was observed that the carbon atoms diffuse from substrate to the surface and react with chromium, which is carried by halide vapors from packing powders and deposited on steel surface, to form chromized coatings. The coatings were mainly composed of chromium carbides, and the performances of these coatings are somewhat dependent on the amount of carbon in substrates. Steels contain the higher carbon concentration, the larger qualities of chromium carbides were produced in chromized coatings leading to better properties.

According to our survey of literatures, there is no similar research has been done in reforming chromized coatings on AISI 1045 carbon steel for the application of bipolar plates. The mate-

* Corresponding author. Tel.: +886 3 3891716; fax: +886 3 3892494.
E-mail address: cybai@ccit.edu.tw (C.-Y. Bai).

0378-7753/$ – see front matter © 2009 Elsevier B.V. All rights reserved.
doi:10.1016/j.jpowsour.2009.08.036

Table 1
Chemical composition of the AISI 1045 steel.

Fe	C	Si	Mn	P	S	Cr	Ni	Mo
Bal.	0.467	0.257	0.750	0.011	0.008	0.017	0.013	0.002

rial is low cost, high strength, and easy to shape into sheets, and therefore was chosen as the substrate of bipolar plates in this work. However, the poor corrosion resistance of the steel has to be improved. This study addresses characteristics of the corrosion resistance and interfacial contact resistance of the steel through pack chromization with an activated pretreatment of rolling or electrical discharge machining for the application of bipolar plates in PEMFC. In addition, the rolling technique was first used as an activated pretreatment to enhance the diffusivity of Cr during chromization, and the performance of rolling pretreatment is compared to that of an electrical discharge machining process.

2. Experimental

2.1. Pretreatment and pack chromization

The raw material used in this work was commercial AISI 1045 steel with a nominal composition as shown in Table 1. Specimens were carried out by rolling or electrical discharge machining pretreatment and cut into the dimensions of 30 mm × 30 mm × 2 mm. Then, SiC abrasive papers were used to grind the original and rolling materials. The pack powder mixture used as chromizing deposition source contained a master metal (Cr), an activator (NH_4Cl) and inert filler (Al_2O_3). The powder mixture was mixed up in accordance with a suitable proportion and homogenized using ball mill for 12 h. The specimens were buried in pack powders filled in a cylindrical alumina crucible and then tightly cover the asbestos on the top of powder. The pack was heated from room temperature to 150 °C at a rate of 10 °C min^{-1} and then held at the temperature for 1 h, then enhanced the temperature to 700 °C and held for 2 h or 4 h. Various chromized coatings have been simply named, and the specimen names and corresponding conditions are shown in Table 2.

2.2. Microstructure and composition analysis

Scanning electron microscope (SEM) was manipulated to analyze microstructures and morphologies of coatings. The crystalline structures and constituent phases of coatings were examined by using X-ray diffraction (XRD) with Cu Kα radiation of λ = 0.15405 nm over a scanning range from 30° to 70°. The distribution of Cr, Fe, C, and N in chromized coatings was assessed with electron probe X-ray micro-analyzer (EPMA). In addition, to identify the elemental concentration on the shallow layer of coatings, the concentration profiles of non-polarized specimens were investigated via X-ray photoelectron spectrometry (XPS).

Table 2
Specimen names and corresponding conditions.

Specimen name	Substrate	Chromization temp. and duration
1045	1045 carbon steel	–
1045-Cr(700-2)	1045 carbon steel	700 °C, 2 h
1045-EDM-Cr(700-2)	EDM-1045 steel	700 °C, 2 h
1045-R-Cr(700-2)	Rolling-1045 steel	700 °C, 2 h
1045-Cr(700-4)	1045 carbon steel	700 °C, 4 h
1045-EDM-Cr(700-4)	EDM-1045 steel	700 °C, 4 h
1045-R-Cr(700-4)	Rolling-1045 steel	700 °C, 4 h

2.3. Electrochemical test

The direct current potentiodynamic and potentiostatic tests were conducted to evaluate the electrochemical behavior of bare steel and chromized specimens with a pretreatment of rolling or electrical discharge machining through a three electrode cell connected to a potentiostate system. A saturated calomel electrode (SCE) was used as a reference to measure the potential across the electrochemical interface. The potentiodynamic test was carried out in a 0.5 M H_2SO_4 solution at room temperature without purging any gases and was measured at the sweeping potential range from −0.5 V to 0.8 V with a scanning rate of 0.5 mV s^{-1}. The potentiostatic polarization measurements were executed at simulated anode (around $-0.1\ V_{SCE}$) and cathode (around $+0.6\ V_{SCE}$) conditions in a 0.5 M H_2SO_4 solution purged with H_2 and O_2, respectively, at 80 °C for 1 h. Before the tests, all specimens were degreased and rinsed with deionized water. Fresh corrosion bath was used for each new specimen.

2.4. Interfacial contact resistance measurement

Measurement techniques for interfacial contact resistance had been well documented in previous literatures [12,13]. In the work, the interfacial contact resistance between the specimen and gas diffusion layer (GDL) was evaluated by a method similar to the report by Wang et al. [3]. As illustrated in Fig. 1, the measured total resistance (R_{T1}) consisted of resistances of bipolar plate (R_{BPP}), two GDLs ($2R_{GDL}$), two copper plates ($2R_{Cu}$), and four interfacial components: two bipolar plate/carbon paper ($2R_{GDL/BPP}$) and two carbon paper/copper plate ($2R_{Cu/GDL}$) interfaces. The R_{T1} is expressed as follows:

$$R_{T1} = 2R_{Cu} + 2R_{Cu/GDL} + 2R_{GDL} + 2R_{GDL/BPP} + R_{BPP} \quad (1)$$

Eq. (2) was performed by measuring the resistance (R_{T2}) of one carbon paper placed between two copper plates without bipolar plates. The resistance of the GDLs could be neglected since the bulk resistance of GDLs is very small, and then two interfacial contact resistance between bipolar plate and GDL can be calculated by subtracting those values from the total resistance (R_{T1}) measured with the metal bipolar plate in place (listed in Eq. (3)):

$$R_{T2} = 2R_{Cu} + 2_{Cu/GDL} + R_{GDL} \quad (2)$$

$$2R_{GDL/BPP} = R_{T1} - R_{T2} - R_{BPP} \quad (3)$$

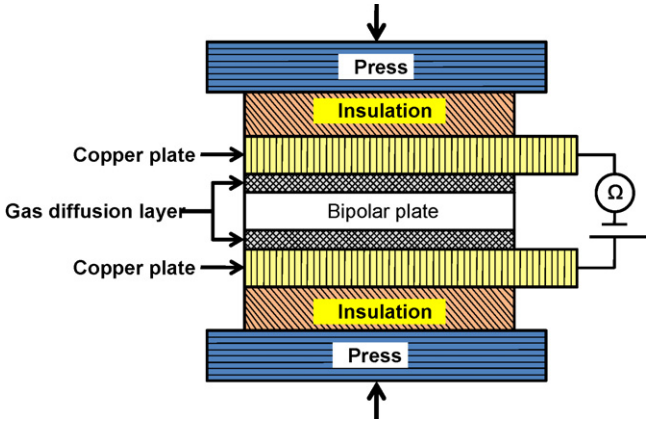

Fig. 1. The schematic of interfacial contact resistance measurement setup.

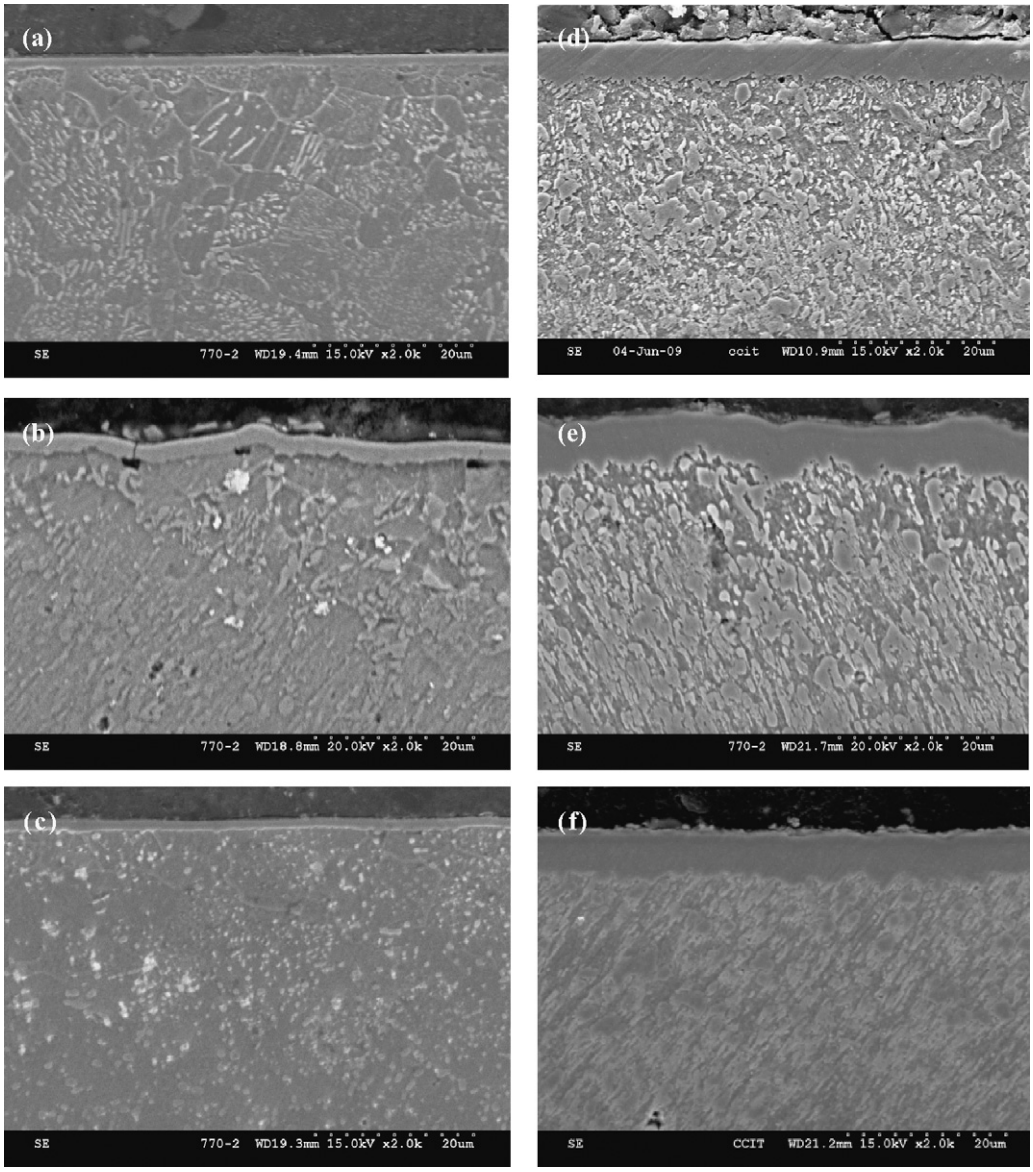

Fig. 2. Cross-sectional SEM images of 1045 steels conducted by low-temperature pack chromization. (a) 1045-Cr(700-2), (b) 1045-EDM-Cr(700-2), (c) 1045-R-Cr(700-2), (d) 1045-Cr(700-4), (e) 1045-EDM-Cr(700-4), and (f) 1045-R-Cr(700-4).

3. Results and discussion

3.1. Microstructure and composition

In order to identify the thickness and microstructure of coatings, various coated specimens were mounted, polished and etched in the solution (5% HNO_3 and 95% C_2H_5OH) for 40 s before observation. Cross-sectional SEM micrographs of the chromized specimens, shown in Fig. 2(a)–(f), indicate that an obvious and continuous chromized layer was deposited on the substrate. Comparing Fig. 2(a)–(c) with (d)–(f), it can be clearly found that the thickness of coatings with activated pretreatment (rolling and electrical discharge machining) was larger than that of non-activated pretreatment. The structures beneath the coatings are pearlite phase, which include α-Fe (dark) and Fe_3C (white). The benefits of chromized process with electrical discharge machining pretreatment are that the high carbon concentration in recast layer can enhance the characterization and thickness of diffusion coatings with carbides during chromization process. Additionally, large amounts of crystalline defects will offer the activation energy or the driving force for enhancing solid diffusion and deposition rates of coatings [11,14,15]. For that reason, the chromization temperature had been effectively lowered to 700 °C. In this study, it is interesting to note that a combination of rolling work and low-temperature pack chromization can generate a similar outcome as that of electrical discharge machining pretreatment. During the

Table 3
The thickness and evaluated characteristics of various chromized coatings measured in the same conditions.

Specimens	Parameters		
	Thickness (μm)	I_{corr} (A cm^{-2})	E_{corr} (V)
1020-Cr(700-2)	0.78	1.24E−06	−0.35
1045-Cr(700-2)	1.18	6.63E−07	−0.06
1045-EDM-Cr(700-2)	3.79	2.21E−07	0.04
1045-R-Cr(700-2)	1.52	3.13E−08	0.02
1045-Cr(700-4)	4.24	9.32E−07	−0.27
1045-EDM-Cr(700-4)	6.04	2.86E−08	−0.07
1045-R-Cr(700-4)	5.84	3.0E−08	0

rolling process, severe plastic deformation leads to the formation of an extremely high density of dislocations and even large amounts of new grain boundaries, which may serve as numerous fast diffusion "channels" for Cr atoms. Actually, the grain boundaries formed via plastic deformation are usually in non-equilibrium states [16] that are associated with a higher stored energy or a higher density of defects compared to the equilibrium grain boundaries in conventional coarse-grained materials. In other words, the non-equilibrium grain boundaries in the specimen possesses a higher Gibbs free energy than the conventional grain boundaries, which may facilitate Cr atoms to diffuse along grain boundaries by decreasing the defect formation energy [17]. Hence, the diffusivity of Cr in the specimens pretreated with rolling work is apparently enhanced when it is compared to that of non-activating treatment regardless of chromization time. Cross-sectional SEM images shown in Fig. 2 also reveal that microstructures of specimens produced by low-temperature pack chromization for 2 h are similar to that of 4 h treatment. However, it was observed that

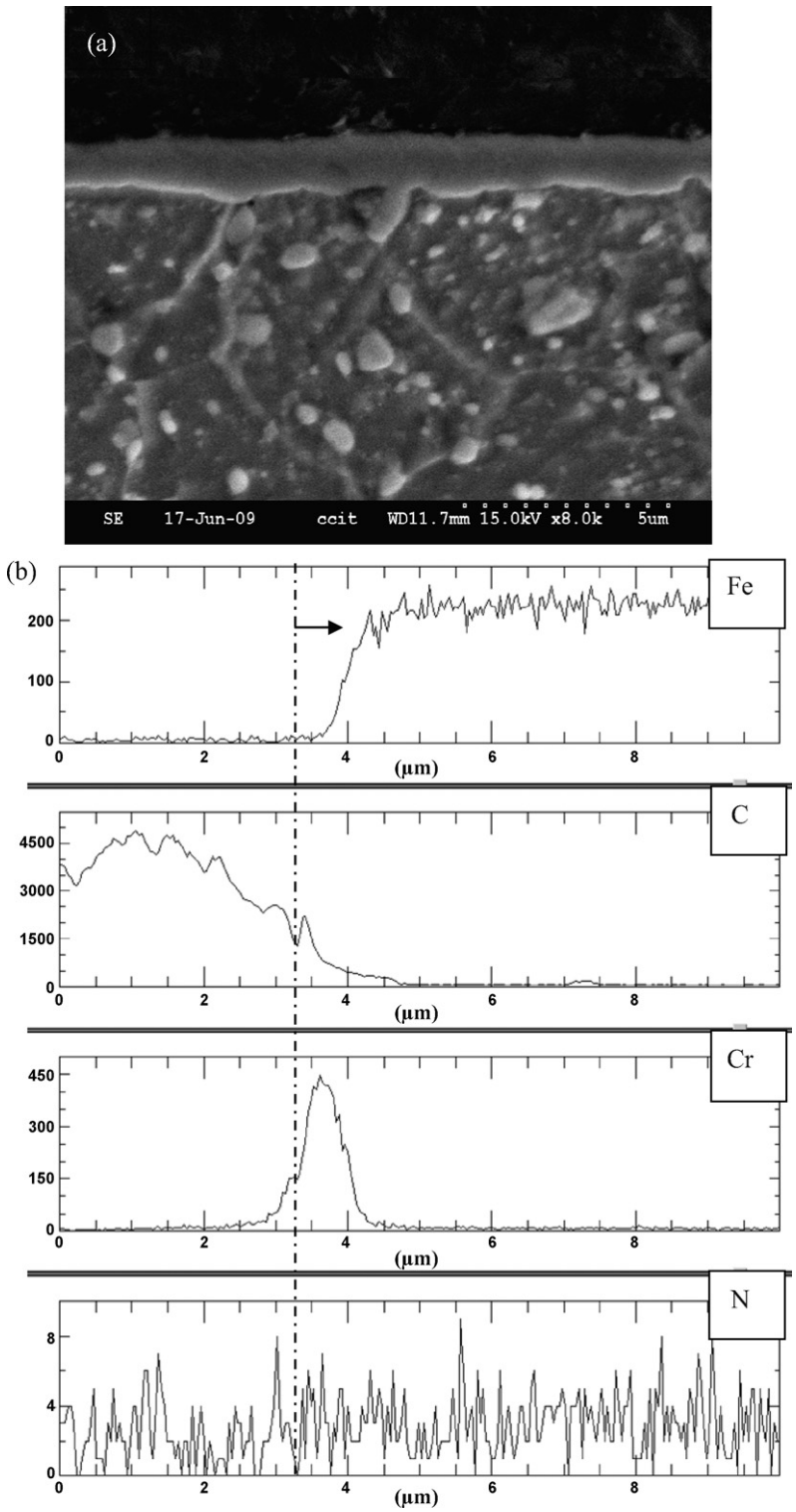

Fig. 3. (a) Cross-sectional SEM micrograph of 1045-R-Cr(700-2), and followed by (b) EPMA line scan of Fe, C, Cr, and N in (a).

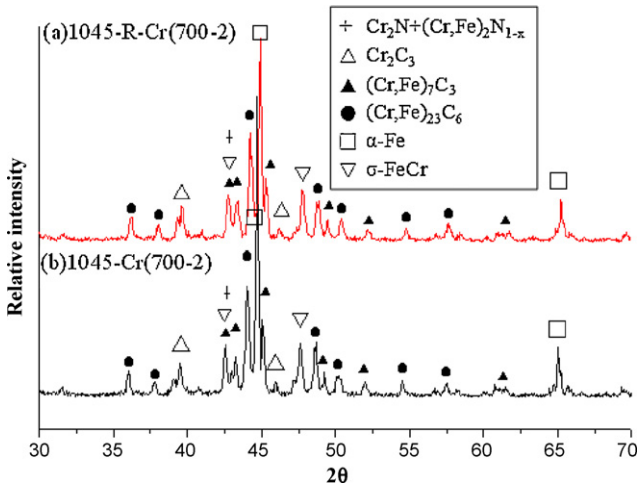

Fig. 4. XRD patterns of (a) 1045-R-Cr(700-2) and (b) 1045-Cr(700-2) coatings.

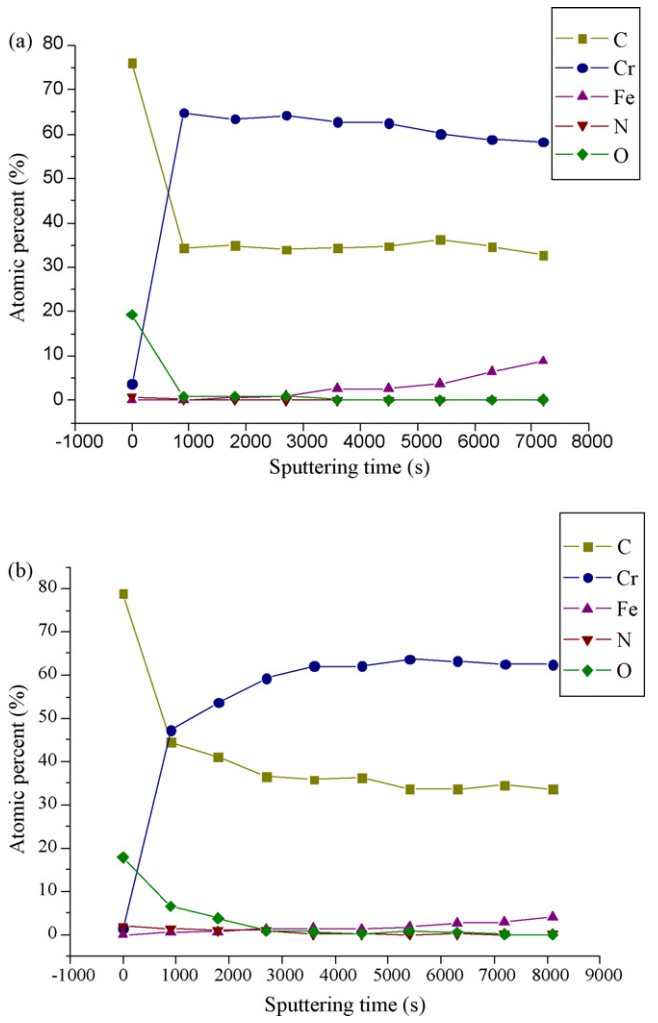

Fig. 5. XPS depth profiles of (a) 1045-R-Cr(700-2) and (b) 1045-EDM-Cr(700-2). The estimated sputtering rate was 1 Å s^{-1}.

the coating thickness drastically increases as well with an advance of operation time. Table 3 shows the thickness of coatings which were chromized with different pretreatment for 2 h and 4 h. The thickness of chromized coating with the pretreatment of electrical discharge machining is larger than that of rolling pretreatment for 2 h operation, but the result did not show the same tendency when increasing the chromization time to 4 h owing to the different amount of rolling work on 1045 steels. Furthermore, the coating thickness of the 1020-Cr(700-2) [11] and 1045-Cr(700-2) are 0.78 μm and 1.18 μm, respectively. In other words, the 1045 carbon steel is more appropriate for low-temperature pack chromization than 1020 carbon steel under the same condition. The cross-sectional micrograph with elemental line scan of 1045-R-Cr(700-2), shown in Fig. 3, exhibits that the coating contains a significant amount of Cr-carbide and a little amount of Cr-nitride distributing near the surface of coating. However, the signal of nitrogen element is not evident, may be most of nitrides centralizing in superficial sites of the coating that were hard to detect by electron beam technique. Fig. 4 represents glancing angle XRD results of 1045-Cr(700-2) and 1045-R-Cr(700-2) indicating that the primary products in these coatings are carbides, including (Cr, Fe)$_{23}C_6$, (Cr, Fe)$_7C_3$, and Cr_2C_3, but a minor product (Cr, Fe)$_2N_{1-x}$ phase is also detected in these specimens. Fe acts as a dopant to the phase of Cr-carbides and nitrides in the deposits. The XPS was conducted to examine the superficial composition of the coatings. Fig. 5 shows the XPS elemental depth profile of 1045-R-Cr(700-2) and 1045-EDM-Cr(700-2) coatings. It is obviously found that the concentration of N is somewhat higher than Fe and only distribute in the shallow layer of coating, which is consistent with the phase analysis of the coatings in XRD, and further confirms that considerable quantities of Cr-carbide as well as little amount of Cr-nitride can be produced simultaneously by low-temperature pack chromization. In addition, comparing Fig. 5(a) with (b), the depth profiles of 1045-R-Cr(700-2) and 1045-EDM-Cr(700-2) are slightly different. A longer time is needed to sputter off the oxygen concentration from the coating of 1045-EDM-Cr(700-2) than that of 1045-R-Cr(700-2). It suggests that 1045-EDM-Cr(700-2) has thicker oxide distribution than that of 1045-R-Cr(700-2), which may strongly affect the values of interfacial contact resistance of these specimens.

3.2. Potentiodynamic test results

The anode potentiodynamic polarization of 1045 steels without and with pretreated and chromized coatings were carried out in a 0.5 M H_2SO_4 solution at room temperature. The polarization curves and the evaluated characteristics of various chromized coatings measured in the same conditions were shown in Fig. 6 and Table 3, respectively. It is noted that all of the coatings deposited with the low-temperature pack chromization show a passivation behavior in such environment. In general, the bipolar plate materials that are suitable for transportation applications should possess superior corrosion resistance, when the fuel cell system are operated at anode potential of −0.1 V and cathode potential of 0.6 V. The cathode potential around 0.6 V was marked in Fig. 6 to simulate the operation conditions of PEMFC. To compare the influence of chromized times on corrosion behaviors, Fig. 6(a) gives the polarization results for the chromization steels of 2 h, and the polarization curves for the chromization steels of 4 h were plotted in Fig. 6(b). In Fig. 6(a), it is obvious that the passivation current for 1045-R-Cr(700-2) specimen is lower than other specimens. The corrosion current density (I_{corr}) of all tested specimens are in the order of bare 1045 > 1045-Cr(700-2) > 1045-EDM-Cr(700-2) > 1045-R-Cr(700-2). In other words, the 1045-R-Cr(700-2) exhibits the best corrosion resistance among all tested specimens. Furthermore, the corrosion potential (E_{corr}) of 1045-EDM-Cr(700-2) and 1045-R-Cr(700-2) are 0.04 V and 0.02 V, respectively. Although the E_{corr} are slightly different, these values are higher than that of bare and simple chrimized steels. Based on the polarization results, it was verified that the rolling pretreatment associated with low-temperature pack chromiza-

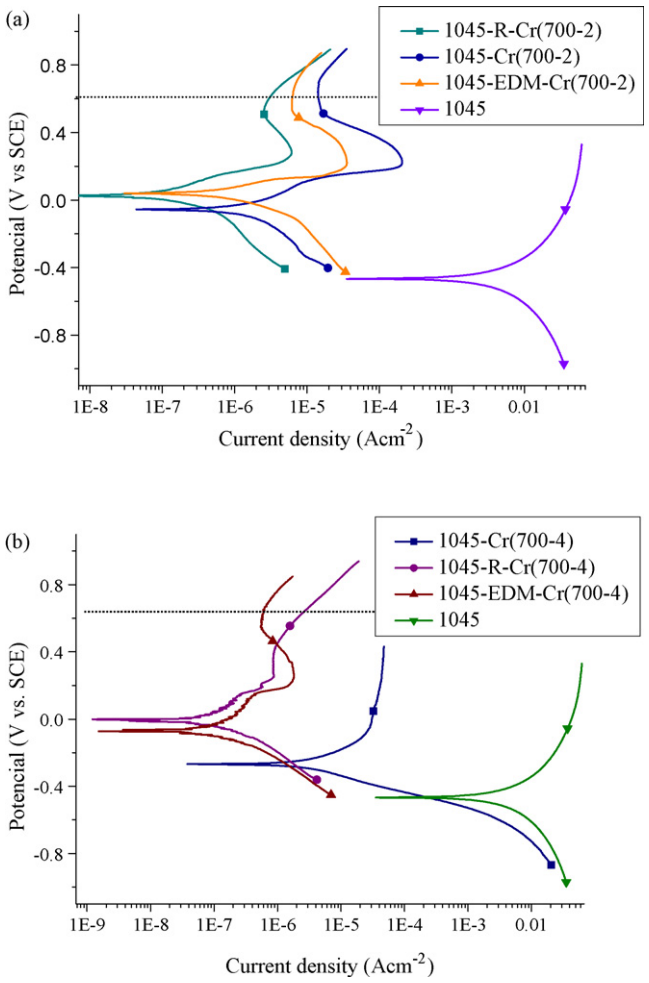

Fig. 6. Polarization curves of bare steels and various chromized steels prepared by pack chromization at 700 °C for (a) 2 h and (b) 4 h, which were measured in a 0.5 M H_2SO_4 solution at 25 °C.

tion could notably enhance the corrosion resistance of carbon steels.

The purpose of increasing chromization duration is expected to attain a thicker chromized coating and upgrade its corrosion resistance. Comparing Fig. 6(a) with (b), it is noticed that the corrosion current density of 1045-EDM-Cr(700-2), 2.22×10^{-7} A cm^{-2}, is higher than that of 1045-EDM-Cr(700-4), 2.86×10^{-8} A cm^{-2}, about one order magnitude. Since micro-cracks produced by electrical discharge machining procedure could be healed through low-temperature pack chromization for a longer duration of heat treatment, the corrosion resistance of these processing steels can be substantially improved by elongating chromization time. However, the corrosion current densities of rolling-chromized steels are very low and not drastically changed with the increasing chromization duration. It supposes that both 1045-R-Cr(700-2) and 1045-R-Cr(700-4) are extremely dense and continuous and possess superior corrosion resistance in this testing environment. In other words, the chromization duration of 2 h is enough to produce an effectively protective coating on 1045 carbon steels with rolling pretreatment. Elongating chromization time to 4 h could not further facilitate the anti-corrosion property of rolling carbon steels, but increase the fabricating cost of chromized coatings.

In comparison to the measurement of the corrosion current density on 1020-Cr(700-2) and 1045-Cr(700-2) in the same testing conditions, which is shown in Table 3. The I_{corr} value of the 1045-Cr(700-2), 6.63×10^{-7} A cm^{-2}, is less than that of 1020-Cr(700-2), 1.24×10^{-6} A cm^{-2}. Additionally, the E_{corr} value of the 1045-Cr(700-2), −0.06 V, is higher than that of 1020-Cr(700-2), −0.35 V. Hence, chromized 1045 steels possess better corrosion resistance and more potential to be candidate material than that of chromized 1020 steels, which is in accordance with previous assumption stating in Section 1.

3.3. Potentiostatic test results

To investigate the corrosion resistance of stainless-steel bipolar plates in simulated anode and cathode environment of PEMFC, Wang and Northwood had studied the effects of O_2 (in cathode environment) and H_2 (in anode environment) on the corrosion behavior of 316L bipolar plates by potentiostatic tests in a 0.5 M H_2SO_4 solution at 70 °C [18]. The test found that the concentration of metal ions in the solution of simulated cathode is much higher than that of anode, and the corrosion level of bipolar plates in cathode environment is more severe than that of anode environment. It explicates clearly that the corrosion resistance of bipolar plates in a cathode environments is worth to pay much attention. The potentiostatic curves of the bare, 1045-Cr(700-2), 1045-EDM-Cr(700-2), and 1045-R-Cr(700-2) steels measured at 0.6 V in a 0.5 M H_2SO_4 solution with oxygen bubbling at 80 °C for 1 h are shown in Fig. 7. The potentiostatic curve of untreated SS410 cited from the literature [19], which was measured under the same condition, is also shown in this figure. It can be seen that the corrosion current density is in the order of 1045 > 1045-Cr(700-2) > SS410 > 1045-EDM-Cr(700-2) > 1045-R-Cr(700-2). A substantial improvement in corrosion resistance of 1045 steel by low-temperature pack chromization with rolling pretreatment can be realized, which is consistent with the potentiodynamic test results. It was observed that the corrosion current density of 1045-EDM-Cr(700-2) rises gradually after the testing time of 1500 s, because there are many micro-cracks caused by electrical discharge machining process existing in the coatings, which can be observed in Fig. 2(b). The thickness of chromized layer is thin relatively in the crack region. Thus, even though the corrosion current density of 1045-EDM-Cr(700-2) is stable at testing duration from initial stage to 1500 s, the thin chromized layer beneath the cracks cannot protect the steel from attack after long-term exposure in the simulated PEMFC environments. On the other hand, although the corrosion current densities of 1045-R-Cr(700-2) are slightly fluctuated with prolonging polarization time, a stable current density about 8.75×10^{-5} A cm^{-2}

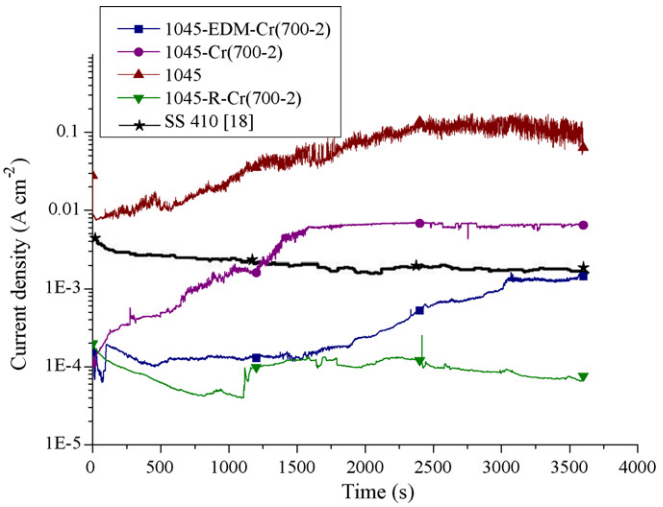

Fig. 7. Potentiostatic curves of the bare, 1045-Cr(700-2), 1045-EDM-Cr(700-2), 1045-R-Cr(700-2), and SS410 steels measured at cathode conditions.

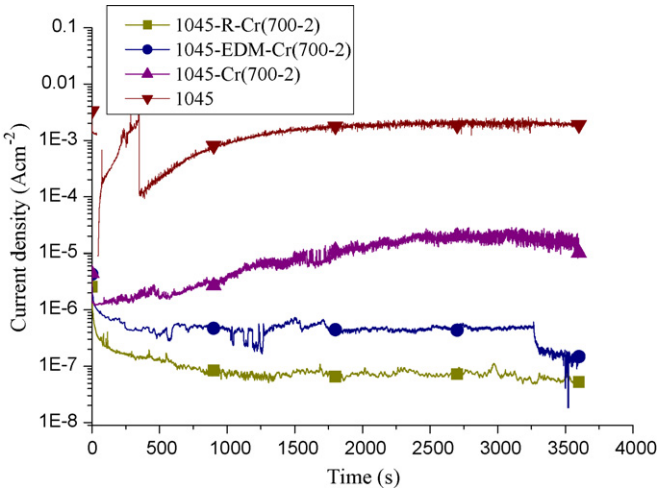

Fig. 8. Potentiostatic curves of the bare, 1045-Cr(700-2), 1045-EDM-Cr(700-2), and 1045-R-Cr(700-2) specimens measured at anode conditions.

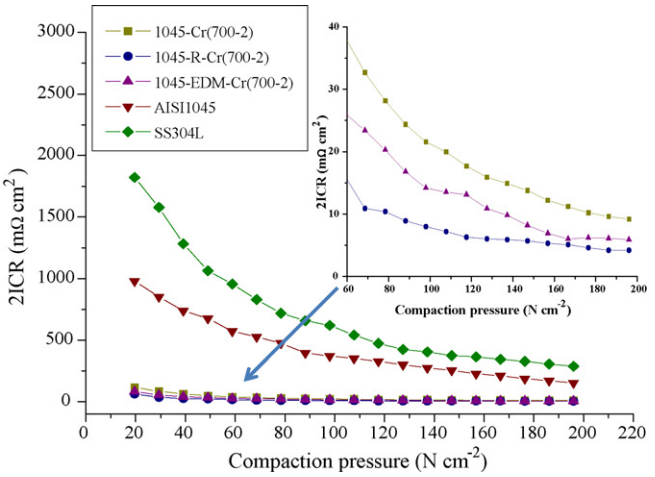

Fig. 9. Interfacial contact resistances between the bipolar plates and carbon papers at various compaction pressures.

is still maintained after 40 min exposure. In addition, the 1045-EDM-Cr(700-2) and 1045-R-Cr(700-2) specimens display better corrosion resistance than the commercial stainless steel SS410. In order to verify the literature mentioned above, the potentiostatic test at anode condition is also conducted and the testing results are shown in Fig. 8. The ranking of corrosion current density in anode condition is 1045 > 1045-Cr(700-2) > 1045-EDM-Cr(700-2) > 1045-R-Cr(700-2), which exhibit the same tendency as that of cathode condition. However, the corrosion current density of all specimens at anode condition is lower than that of the cathode condition. It indicates that corrosion degrees of the specimens at anode environment are slighter than that of cathode environment, which is consistent with the statement of the literature. Specifically, the corrosion current density of 1045-R-Cr(700-2) and 1045-EDM-Cr(700-2) at simulated anode condition displays very small values of 7.56×10^{-8} A cm^{-2} and 1.22×10^{-7} A cm^{-2}, respectively. Hence, the results provide a convincing evidence to verify the benefit effect of the chromium-carbide coatings yielded by low-temperature pack chromization with electrical discharge machining or rolling pretreatment on protecting bipolar plates against the corrosion attack in a simulated PEMFC environment.

3.4. Interfacial contact resistance test

Interfacial contact resistances between the steels, with and without coatings, and gas diffusion layers as a function of compaction pressures are shown in Fig. 9. For comparing the superficial conductivity of the chromized steels with commercial stainless steels, the value of interfacial contact resistance for the untreated 304L, measured under the same conditions, is also shown in this figure. The contact resistance values of all measured specimens decrease with increasing compaction pressure. The values of SS 304L are the highest among all tested specimens due to the formation of passive layer on the surface. Refer to previous studies [20–23], composition and roughness of the coating are the main factors to affect the interfacial contact resistance. The specimens with coatings produced by pack chromization possess lower contact resistance values than that of SS 304L, because the chromium carbide generated via pack chromization has the better conductivity than that of chromium oxide. In addition, the XRD results (Fig. 4) represent that little amounts of chromium nitride doping with Fe were also found in the chromized coatings, which contribute to high conductivity of the coatings as well [24]. The contact resistance values of the specimens treated by low-temperature pack chromization are in the order of 1045-Cr(700-2) > 1045-EDM-Cr(700-2) > 1045-R-Cr(700-2). Moreover, the ICR values of 1045-Cr(700-2), 1045-EDM-Cr(700-2), and 1045-R-Cr(700-2) are 14.9 mΩ cm^2, 9.8 mΩ cm^2, and 5.9 mΩ cm^2, respectively, which all achieve the goal of U.S. DOE for bipolar plate application. According to previous study of the literature [25], the contact resistance between bipolar plates and gas diffusion layers can be effectively decreased by texturing the surface roughness of bipolar plates to a suitable range, which is close to the surface roughness of gas diffusion layers. The surface roughness of 1045-R-Cr(700-2) and 1045-EDM-Cr(700-2) measured by a profilometer is 0.11 μm and 3.67 μm, respectively. It is clear that the surface roughness of 1045-EDM-Cr(700-2) is larger than that of 1045-R-Cr(700-2). However, the contact resistance values of 1045-R-Cr(700-2) are smaller, although the surface roughness of 1045-EDM-Cr(700-2) is near to that of a carbon paper (gas diffusion layer). In fact, the interface contact resistance between bipolar plates and gas diffusion layers is dependent on not only the surface roughness but also the superficial composition of bipolar plates. As can be seen in Fig. 5, the oxygen concentration of 1045-EDM-Cr(700-2) is higher than that of 1045-R-Cr(700-2) in a superficial scope (about 300 nm). It indicates that the 1045-EDM-Cr(700-2) contains larger amounts of metal oxide, which possess poor conductivity, than the 1045-R-Cr(700-2). Therefore, the superficial electrical conductivity of 1045-EDM-Cr(700-2) is lower than that of 1045-R-Cr(700-2), and the contact resistance value of 1045-R-Cr(700-2) is lower. The results of interfacial contact resistance tests reveal that the effect of surface composition of bipolar plates on contact resistance between bipolar plates and gas diffusion layers is greater than surface roughness.

4. Conclusion

Low cost AISI 1045 steels with various chromized coatings, prepared by activating pretreatment and low-temperature pack chromization, were tested and evaluated to act as an alternative material for PEMFC bipolar plates. The polarization results show that the 1045-R-Cr(700-2) specimen exhibits the lowest corrosion current density, 3.13×10^{-8} A cm^{-2}, in the potentiodynamic testing. Additionally, the 1045-R-Cr(700-2) specimen has the most stable corrosion current, 7.56×10^{-8} A cm^{-2} at anode condition and 8.75×10^{-5} A cm^{-2} at cathode environment, in the potentiostatic testing. The polarization results show that the 1045-R-Cr(700-2) specimen exhibits the lowest corrosion current density, 3.13×10^{-8} A cm^{-2}, in the potentiodynamic testing and the

most stable corrosion current, 8.75×10^{-5} A cm^{-2}, in the potentiostatic testing, respectively. In the view of corrosion resistance, the coatings prepared by rolling and chromization for 2 h possess excellent performance, but the anti-corrosion property of rolling-chromization coatings could not be further improved by extending the chromization time. However, the corrosion resistance of chromized specimen with the pretreatment of electrical discharge machining can be significantly promoted with increasing the chromization duration from 2 h to 4 h. Furthermore, all the chromized specimens have a lower interfacial contact resistance than that of both bare 1045 carbon steel and 304L stainless steel, and the 1045-R-Cr(700-2) possess the lowest contact resistance values, 5.9 mΩ cm^2, among chromized specimens. Hence, the performance of chromized carbon steels is comparable to that of graphite or noble metals for the application of bipolar plates in PEMFC, but the fabricating or material cost of graphite or noble metals is much higher than that of chromized carbon steels. In this sense, the method of low-temperature pack chromization associated with rolling technique represents an idea and result for manufacturing a low cost and effective bipolar plate. The current efforts are to use the chromized carbon steels as bipolar plates on the investigation of actual single cells and the corresponding properties of the cells will also be studied in our future work.

Acknowledgment

This work was sponsored by National Science Council of Republic of China under Grant No. NSC 97-2221-E-606-004.

References

[1] H. Tawfik, Y. Hung, D. Mahajan, J. Power Sources 163 (2007) 755–767.
[2] V. Metha, J.S. Cooper, J. Power Sources 114 (2003) 32–53.
[3] H. Wang, M.A. Sweikar, J.A. Turner, J. Power Sources 115 (2003) 243–251.
[4] C.Y. Bai, Y.H. Chou, C.L. Chao, S.J. Lee, M.D. Ger, J. Power Sources 183 (2008) 174–181.
[5] J. Wind, R. Spah, W. Kaiser, G. Bohm, J. Power Sources 105 (2002) 256–260.
[6] S.J. Lee, C.H. Huang, J.J. Lai, Y.P. Chen, J. Power Sources 131 (2003) 243–257.
[7] S.H. Wang, J.C. Peng, W.B. Lui, J. Power Sources 160 (2006) 485–489.
[8] V.V. Nikam, R.G. Reddy, J. Power Sources 152 (2005) 146–155.
[9] T.H. Wang, L.L. Seigle, Mater. Sci. Eng. A 108 (1989) 253–263.
[10] L. Levin, A. Ginzburge, L. Klinger, T. Werber, A. Katsman, P. Schaaf, Surf. Coat. Technol. 106 (1998) 209–213.
[11] C.Y. Bai, M.D. Ger, M.S. Wu, Int. J. Hydrogen Energy doi:10.1016/j.ijhydene.2009.05.103, in press.
[12] D.P. Davies, P.L. Adcock, M. Turpin, S.J. Rowen, J. Power Sources 86 (2000) 237–242.
[13] S.J. Lee, C.H. Huang, J.J. Lai, Y.P. Chen, J. Power Sources 131 (2004) 162–168.
[14] K. Lu, J. Lu, Mater. Sci. Eng. A: Struct. 375–377 (1–2) (2004) 38–45.
[15] Z.B. Wang, J. Lu, K. Lu, Acta Mater. 53 (7) (2005) 2081–2089.
[16] Y.R. Kolobov, G.P. Grabovetskaya, M.B. Ivanov, A.P. Zhilyaev, R.Z. Valiev, Scripta Mater. 44 (2001) 873–878.
[17] Z.B. Wang, N.R. Tao, W.P. Tong, J. Lu, K. Lu, Acta Mater. 51 (14) (2003) 4319–4329.
[18] Y. Wang, D.O. Northwood, Electrochim. Acta 52 (2007) 6793–6798.
[19] Y. Wang, D.O. Northwood, Int. J. Hydrogen Energy 32 (7) (2007) 895–902.
[20] G. Lin, A.J. Shih, S.J. Hu, J. Power Sources 163 (2007) 777–783.
[21] A. Kraytsberg, M. Auinat, Y. Ein-Eli, J. Power Sources 164 (2007) 697–703.
[22] H. Wang, M.P. Brady, K.L. More, H.M. Meyer, J.A. Turner, J. Power Sources 138 (2004) 79–85.
[23] A. Pozio, F. Zaza, A. Masci, R.F. Silva, J. Power Sources 179 (2008) 631–639.
[24] H. Wang, M.P. Brady, G. Teeter, J.A. Turner, J. Power Sources 138 (2004) 86–93.
[25] A. Bharat, H. Pradeep, J. Power Sources 188 (2009) 225–229.